Waste-bagasse derived sustainable activated carbons for enhanced deionization and decontamination of drinking water

R. Hayder [a], Z. Anjum [b], M. Khalid [c], R. Riaz [d], S. Mumtaz [c], M. Hafeez [a,*], I. Zaheer [a]

[1] *Department of Chemistry, The University of Azad Jammu and Kashmir, 13100 Muzaffarabad, Pakistan*

[2] *Department of Biotechnology, University of Azad Jammu & Kashmir, Muzaffarabad, 13100, Pakistan*

[3] *Department of Biotechnology, Faculty of Science and Technology, Women University of Azad Jammu and Kashmir Bagh, 12500, Pakistan*

[4] *Department of wildlife biology and conservation Edinburgh Napier university 9 Sighthill Ct, Edinburgh EH11 4BN, United Kingdom*

This study focusing on the removal of inorganic and microbial contaminants from drinking water. The activated carbons (ACs) were synthesized as precursor AC-1, derived from sustainable waste bagasse hydrochars through phosphoric acid activation, exhibits substantial antibacterial properties and a significant specific surface area of 1460 m^2/g. The AC-1 was immobilized with FeS (AC-FeS), demonstrates remarkable efficiency in removing (F^-), (NO_3^-), and gram-negative bacteria from drinking water, outperforming previous methods under dynamic conditions. Optimized removal for NO_3^- and F^- reached 94% and 92%, respectively with 100% bacterial removal within 6 hours. The bacterial decontamination closely adhered to the Langmuir kinetics.

(Received February 14, 2025; Accepted May 27, 2025)

Keywords: Sustainable activated carbon (AC), H_3PO_4 activation, Iron sulfide nanoparticles (FeS), Nitrate and fluoride (F^-/NO_3^-) adsorption, Antimicrobial activity, Sustainable development goals of UN

1. Introduction

Water pollution, characterized by inorganic and microbial contaminants, is a global crisis impacting human health and environmental sustainability. In the United States, the prevalence of diseases like diarrheal deaths and stomach infections has been linked to high concentrations of aquatic microbes, often surpassing [1] the safety limits set by the World Health Organization and the U.S. Environmental Protection Agency. [2] The situation is even more dire in developing countries, where waterborne diseases annually claim millions of lives due to the presence of harmful bacteria and inorganic pollutants in drinking water. [3] This looming crisis, exacerbated by resource scarcity, predicts that a billion people could lack access to clean water in the coming decades. [4,5] Waterborne diseases, ranging from diarrhea and tuberculosis to ulcers that can evolve into cancers, are often attributed to contaminants like bacteria and nitrates in freshwater bodies. [6] Additionally, issues like fluorosis arise from fluoride in water, underscoring the urgent need for innovative water purification technologies.

Activated carbons (ACs), derived from biomass, have emerged as a promising solution against waterborne pathogens and inorganic pollutants,[7,8] offering an effective technique for purifying drinking water. While other materials like chitosan, [9] nano-silver, [10] titanium dioxide, [11] carbon-based nanomaterials, [12] and iron sulfide nanoparticles[13] have shown potential in water decontamination, the effectiveness of these technologies largely depends on their composition. [14] Recent advancements have highlighted the efficacy of nanotechnology-based solutions, [15,16]

* Corresponding author: smhafeezkhan@yahoo.com
https://doi.org/10.15251/DJNB.2025.202.567

including carbon nanotubes, nanocatalysts, membrane technology, and nano-sorbents, in treating polluted water. In particular, combining nanoparticles with ACs could offer enhanced decontamination capabilities. [17] ACs, known for their large surface area, are ideal substrates for nanoparticle impregnation. Sources like rice husk, [18] coconut shells, [19] and plant biomass, [20] can be tailored with metal nanoparticles for water purification. [21] For instance, iron sulfide nanoparticles have shown significant activity against bacteria,[22] nitrates[23] and fluoride[24] in water, with various studies reporting successful removal of these contaminants using bio-derived ACs. [25-27]

Despite this, developing an effective solution for aqueous pathogens remains a challenge. [28] This paper introduces a novel material with improved dual potential for removing inorganics and microbes from polluted water. This material not only demonstrates a high surface area but is also derived from recyclable sources, making it a robust and sustainable option for water treatment.

2. Experimental

The hydrochar was prepared by drying the waste bagasse at 110°C for 12 hours in a vacuum oven. The products were then crushed and ground into a fine powder. The powdered material (32g) was then filled in an autoclave (50 ml, Sigma Scientific China), using 17.9 ml of distilled water (filling 35.8 % area of the autoclave). The hydrothermal carbonization (HTC) was done at 200°C for 12 hours [29]. The resultant hydrochar was washed thoroughly with deionized water and dried overnight in a vacuum oven at 110°C (Thermo-Scientific Ireland). The hydrochar was activated using an acid (H_3PO_4, Sigma Aldrich) with precursor to acid ration of 1:2 precisely. A weighted amount of 10g of hydrochars were mixed with 14.05g of H_3PO_4 and stirred overnight at 150rpm. Then activation was done at 900°C (5°C /minute) [30], under nitrogen flow (6 mL/min) for 12 hours, to get an activated carbon sample (AC-1). The resultant sample was then washed with deionized water until the pH was stabilized and dried at 110°C overnight in a vacuum oven.

The AC-1 was subsequently impregnated with FeS to prepare AC-FeS using the *insitu* incipient wetness method. FeS micronpowder (Thermo-Scientific USA) was used for impregnation. To synthesize AC-FeS material, the activated material (0.5.g) was mixed with 1.75mmol FeS (using 0.153g of FeS) and stirred overnight. Material was heated in a tube-furnace, at 1200°C in an inert atmosphere for 2 hours to obtain FeS impregnated AC. The AC-FeS was collected, rinsed with deionized water, and left to dry at 110°C overnight in a vacuum oven.

Textural analyses of all samples were performed on Micromeratics ASAP 2020 using nitrogen gas sorption technique after degassing at 300C°. The adsorption models such as Brunauer Emmett-Teller (BET) and density functional theory (DFT) methods used to find specific surface area and microporous volumes. Thermal stability was assessed through Discovery TGA instrument with a ramp of 10C°/minute under air environment. The morphology of the material was analyzed using transmission electron microscopy (TEM, JEOL JEM 2100), the sample was mixed with deionized water and a film is made on a carbon coated grid (400 mesh) and allowed to dry for 40 minutes before going for imaging. Scanning electron microscopy (SEM) instrument was used to obtain SEM-micrographs, taken at JSM-7401F (JEOL, Japan). The instrument has a Schottky-type field emission gun and a secondary electron detector. The working distance was kept at 3 millimeters. The instrument was operated at 0.6 kV accelerating voltage without applying any coating. Dried particles were transferred on carbon coated aluminum substrate before loading in the microscope. Energy dispersive X-rays spectroscopy (EDS) coupled with SEM instrument, provided morphological and compositional insights. Raman (Horiba LabRAM HR 800, laser power of 50mW at laser intensities of 10 per cent and laser wavelength was 535 nm) and inferared spectroscopy (FT-9700, Perkin Elmer, using sample pallets) were employed for molecular characterization, and X-ray diffraction (XRD) analysis was carried out in X'Pert PRO X-ray diffractometer (USA) with Cu-K_α X-ray (λ = 0.15418 nm) ranging from 10° to 80° was used to understand the crystalline/amorphous nature of the materials. Further details of the methods is provided in the supporting information.

The Lovibond's Spectrophotometer (Lovibond XD-7500 Germany) was used to obtain the concentrations of both NO_3^- and F^- ions. Nitra-X kit (Lovibond Germany) was used for NO_3^- analysis and standard SPANDS solution (Lovibond Germany) was used in F^- analysis. The sorption was carried out in both static (unstirred) and dynamic conditions (stirred at 50rpm) but optimum removal

percentages for NO_3^- and F^- were attained under dynamic conditions when AC-FeS was used. 0.1g of the material was used for both NO_3^- and F^- absorption, initial concentrations for both NO_3^- and F^- solutions were 30 ppm and 3.0 ppm each, respectively.

The Miller Lauria Broth was prepared by dissolving 1g of bacto-trypton, 0.5 g of bactoyeast extract and 0.5 g of NaCl (Merck). The reagents were put into an autoclave and sterilized, the reagents were then mixed with freshly prepared 0.2 M glucose solution (prepared in deionized water) and pH was maintained to 6.8 to 7.1 using HCl/NaOH buffer and the filtrate was then incubated at 25°C. The Bile ager was prepared according to manufacturer (Merck) instructions, by using ready to use powdered material. The pH was adjusted to 7.4 ± 0.1 using HCl and NaOH buffers. The medium was boiled for 2 minutes and then stored at 42 ± 2 °C before pouring into plates.

The E. LB medium for *Escherichia coli (E. coli)*) was made to grow the bacterial colonies by combining 5 g of Miller's LB broth with 1000 mL of deionized water. *E. coli* (150 µL) were grown with 3 mL of LB media which was incubated for 3 hours at 160 rpm. *Total. Coliforms (T.Coliforms)* were cultured from bile ager at 37°C overnight. The bacterial population was presented as a colony-forming unit (CFU) value, which was obtained with customized 3M-Petrifilms using a colony counter (Table ST-1). The initial concentration of the bacterial population was 100 colonies/mL. These colonies were further diluted with 10mL distilled water at first and then 1mL from this dilution is further diluted to 10mL of sterile water to obtain 10^2 dilution (1000mL dilution) to enumerate the concentration of both *E. coli* and *T. coliforms*. The decontaminating material was tested against *E.coli* (150 CFU/mg after 10^2 dilutions) and *T.coliforms* (200 CFU/mg after10^2 dilution). Thus, the reference concentrations of both *E.coli* and *T.coliforms* were 150 CFU and 200 CFU before the addition of any de-polluting material.

The spectrophotometer (UV-Visible V-760 (JASCO)) with a photomultiplier detector has been used for the kinetic studies on bacterial removal by AC-FeS. Time spectra were collected between 350 to 750 nm, and kinetic data was obtained at a wavelength of 510 nm to determine the pseudo-first-order rate constants. The rate constants obtained represent the average of three replicated runs.

3. Results and discussion

Our synthesized precursor notably achieved the highest surface area recorded under our experimental conditions topping 1460 m²/g (Figure 1a), despite reports about similar works [31,32]. This increase in surface area enhanced its activity for nitrates (NO_3^-) and fluorides (F-) removal, and gram-negative bacteria, when modified with FeS to form AC-FeS.

The pore size distribution peaked at 3.3 nm and an average pore volume of 0.66 m³/g for AC-1 with a majority texture was microporous with shorter dwell time. In a similar context, Budinova et al. reported analogous findings in their study on H_3PO_4-derived activated carbons, which had a surface area of 900 m²/g and a pore volume of 0.66 m³/g [33]. Furthermore, Srinivasan et al. examined the impact of plasma treatment on activated carbons [34], reporting a minimal increase in the surface area from 415 m²/g to 425 m²/g following plasma treatment. The total pore volumes in these cases were 0.19 m³/g and 0.20 m³/g, respectively.

Table 1. Surface area parameters for AC-1 and AC-FeS from gas sorption experiments.

S_{BET} (m^2/g)	S_{ext} (m^2/g)	S_{micro} (m^2/g)	Pore volume (m^3/g)			Rel-Pore volume		Avg. Pore Diameter(nm)
			V_{total}	V_{micro}	V_{meso}	V_{micro}/V_{total}	V_{meso}/V_{total}	
1460(AC-1)	703	757	0.66	0.30	0.36	45%	55%	3.3
618(AC-FeS)	618	0	0.47	0	0.47	0%	100%	3.0

Table 1. demonstrates a consistent decrease in the surface area of activated carbons (AC-1), which aligns with the results obtained from thermogravimetric analysis (TGA) as detailed in Supplementary Section S-2. To further investigate the morphology of the ACs, SEM analysis was employed. SEM images, as seen in Figure 1b, revealed that the majority of the particles were spherical, with an average size of 0.5 µm. Interestingly, the SEM analysis indicated that the particle morphology was largely retained after heat treatment. It was observed that AC-FeS particles were not dispersed on the outer surface of the ACs. This observation was further corroborated by Energy Dispersive X-ray Spectroscopy (EDS) analysis, which confirmed the presence of iron, sulfur, and oxygen in the synthesized material, as presented in Figure 1(c).

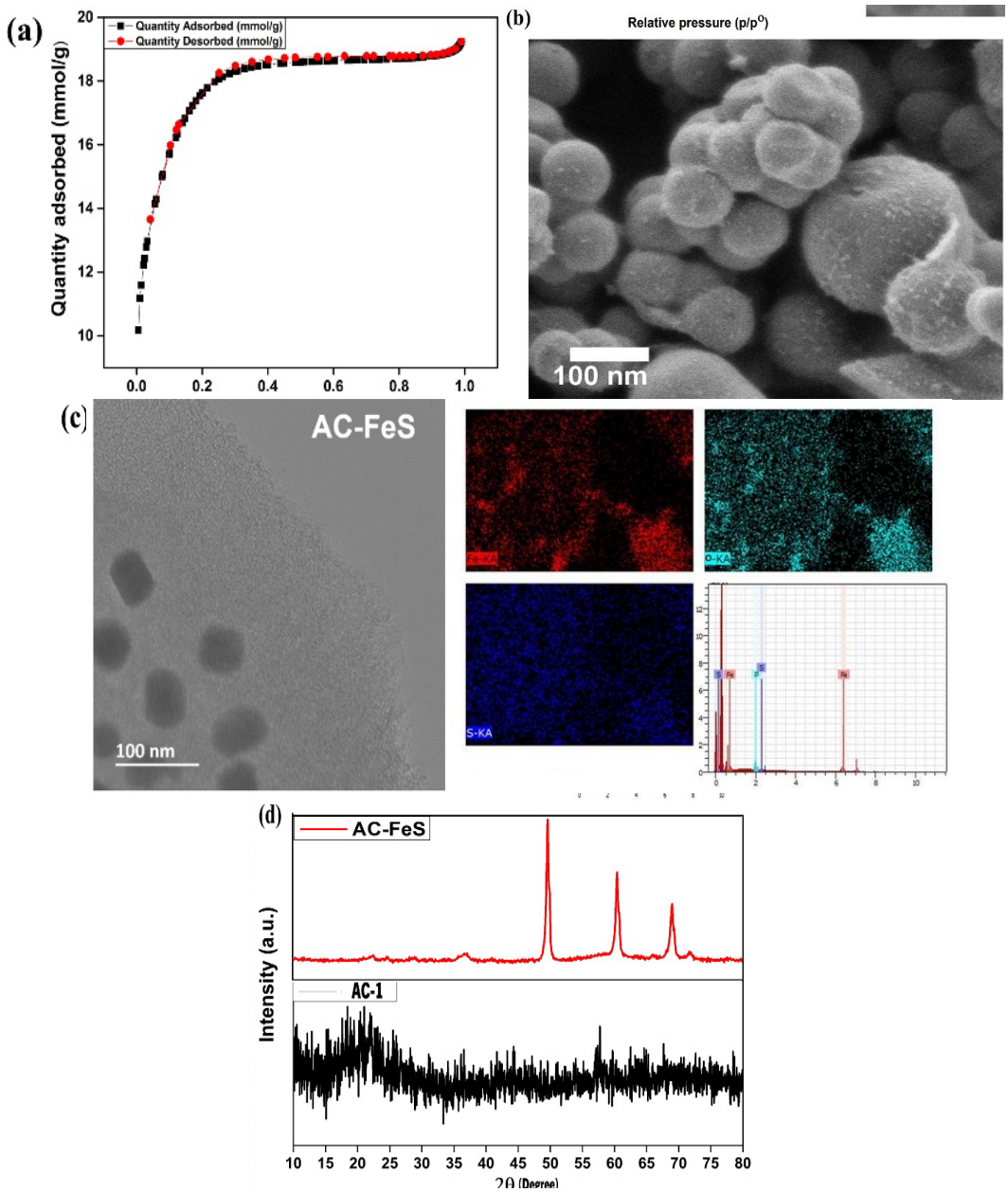

Fig. 2. (a) N_2 adsorption-desorption isotherm shows significant gas adsorption (mmol/g) by AC-1, which is used for antibacterial activity in wastewater. (b) SEM images of FeS-loaded activated carbons with 0.5µ size at high resolution showing no partical dispersion on the surfcae of material evidencing the infilteration of FeS in the activated material. (c) EDS mapping and TEM image of FeS-loaded activated carbons showing the compositional constitution of FeS-loaded activated carbons. (d) The X-ray diffractogram of amorphous activated carbons and FeS-loaded activated carbon.

Complementing these findings, pXRD analysis provided insights into the crystalline structure of the materials. The pXRD diffractogram, shown in (Figure 1d), indicated that AC-1 was primarily amorphous in nature before being tailored with FeS for water decontamination purposes. Post-impgregnation, the AC-FeS samples exhibited distinct crystalline diffraction peaks characteristic of FeS nanoparticles. Specifically, pXRD peaks for FeS were at 37.1°, 47.4°, 60.3°, and 69.1° were associated with the (111), (200), (210), and (311) reflection of the FeS nanoparticles, as per the JCPDS card No. 42-1340. These findings not only confirm the successful incorporation of FeS nanoparticles into the AC structure but also highlighted the transformation of the AC-FeS to a more crystalline state post-modification.

The experiments were conducted under both static and dynamic conditions, utilizing 0.1g of FeS (from the micronpowder) and AC-FeS as sorbent materials. In dynamic conditions with a 100mL water sample, the removal efficiencies achieved using FeS and AC-FeS were notably high: 90% and 94% for nitrate (NO_3^-), and 90% and 92% for fluoride (F-), respectively. In contrast, the precursor AC-1, when tested against fluoride and nitrate, exhibited only minimal adsorption of these ions in both static and dynamic settings. This difference in performance highlights the enhanced adsorption capabilities of AC-FeS, especially under dynamic conditions. Dynamic settings proved more effective due to the improved mixing of the sorbent material with the water, facilitating higher removal rates compared to static equilibrium [35].

Figure 2. presents a comparative analysis of the results under both conditions for AC-1, FeS, and AC-FeS. Notably, the incorporation of iron functionality in the sorbents played a significant role in the removal efficiency. Iron sulfide, being in trace, exhibits a strong affinity towards both fluoride and nitrate ions, effectively scavenging these contaminants from the aqueous solution.

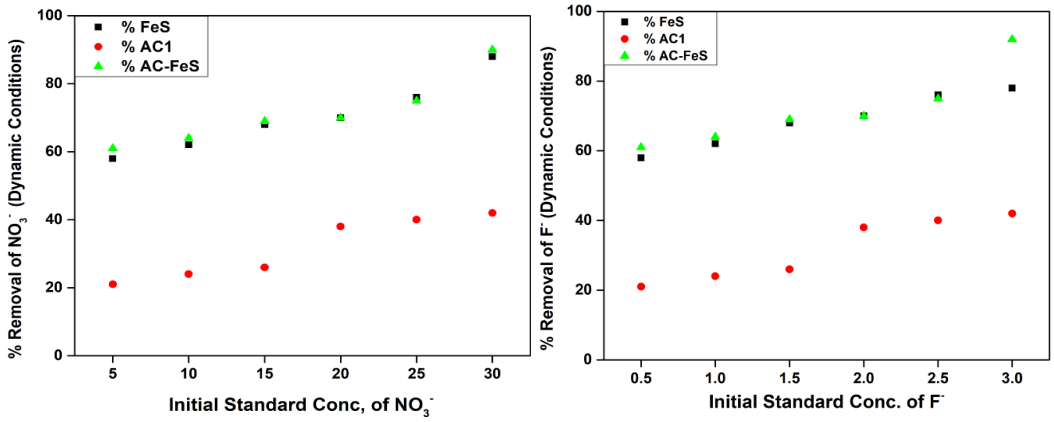

Fig. 3. Comparative analysis of the results under Dynamic conditions for AC-1, FeS, and AC-FeS. Notably, the incorporation of iron functionality in the sorbents played a significant role in the removal efficiency of water contained contaminants.

In this study, we synthesized modified activated carbons loaded with FeS nanoparticles (AC-FeS), demonstrating high efficacy in microbial decontamination. A review of the literature reveals various materials like graphene oxide, [36,37] modified silica, [38] metal oxide nanoparticles, [39] and activated carbons, [40] all possessing antibacterial characteristics. Specifically, our synthesized AC-1 showed significant activity against gram-negative microbes, achieving 35% bacterial removal even without the addition of FeS NPs. Comparatively, Oya et al. reported similar decontamination results using mesoporous activated carbon in freshwater. [41] Zhang et al. demonstrated enhanced antibacterial activity in wastewater systems using ACs loaded with silver nanoparticles (Ag-NPs). [42] Other studies have also confirmed the antibacterial behavior of metal oxide and metal sulfide nanoparticles. [43]

To explore this further, we impregnated FeS NPs into ACs and tested their bacterial removal efficacy. AC-FeS, applied to communal waters contaminated with T. coliforms and E. coli, showed

improved decontamination effectiveness (see Supplementary Text ST-1). The iron sulfide nanoparticles were particularly effective, achieving a 99% removal rate for gram-negative bacteria, in line with literature findings. [44,45] Our approach, using AC-1 as a raw waste starting material, proved more effective and economical. The functional groups in the synthesized material, evidenced by Raman spectroscopy, contributed to its efficiency. The material-maintained its decontamination effectiveness for up to six cycles, though some decrease in depolluting activity was noted (see Supplementary Information SI). The comparative decontamination results for AC1, FeS, and AC-FeS are depicted in Figures 3(a) and (b).

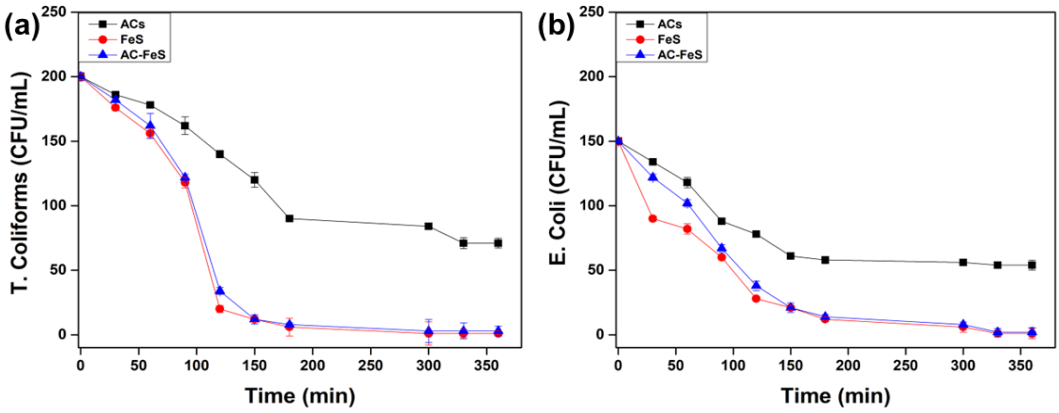

Fig. 4. (a). Response of T. Coliforms vs time (a) and E.Coli vs time (b) after adding 0.1g of AC-1, FeS and AC-FeS, respectively.

The antibacterial mechanism is attributed to the sulfide moiety in FeS, which disrupts bacterial genomes and induces bacterial inactivation. [44,45] Pachaiappan et al., investigated the antibacterial effects of metal (MoS) sulfide nanoparticles in water treatment,[46] and Roy et al., who explored the antibacterial activity of CuS NPs in wastewater. [21] Li et al. and Ajibade et al. have also reported successful bacterial decontamination using FeS nanoparticles.[47,48]. Our study aligns with these findings, showing a consistent decrease in bacterial colonies using FeS NPs. However, when FeS is combined with the sustainable AC-1 to form AC-FeS, we observed an even greater antibacterial efficacy. This improvement could be attributed to factors such as surface functional groups like acids, aldehydes, and lactones [49,50], which enhance the material's decontamination activity in aqueous conditions. In our material too these groups are evidenced in IR-spectrograph (see SI) which show the presence of acid and carbonyl functional groups. Remarkably, our AC-FeS material achieved 100% antibacterial activity against T. coliforms and E. coli. Using 0.1 g of AC-FeS in 1 ml of contaminated water, we monitored the decontamination process, observing a gradual but complete elimination of both bacterial strains within 6 hours.

Table 2. Comparison of the removal percentages of Bacteria and Anions to the literature values.

Material Type	**Contaminant**	**Medium/Removal**	**Ref**
Cu_2S NPs	Bacteria	Water (90%)	**[51]**
FeS nanoparticles	Bacteria	Water	[21]
Metal sulfide particles	Gram Negative Bacteria	Water (80%)	[48]
FeS NPs	Gram Negative Bacteria	Water	[52]
AgO Nanoparticles	Gram Negative Bacteria	Water (0.03%)	[53]
ZnO Nanoparticles	Bacteria	Water (52%)	[54]
FeO NPs	NO_3^-	Water (>90%)	[55]
CeO NPs	F^-	Water (>90%)	[56]

A key feature of the activated carbon was its substantial specific surface area of 1460 m^2/g, that helped towards the enhanced antibacterial activity of the material under study along with the removal of F^- and NO_3^- from drinking water. While numerous studies have explored the antibacterial activities of modified ACs, this study distinctively highlights the enhanced pollutants removal capacity of AC-FeS from water, attributed to the effective impregnation of FeS within the ACs.

We investigated the kinetics of antibacterial activity using AC-FeS at a pH of 7.1 and temperature of 25°C, employing spectral measurements for analysis. The kinetics data revealed that the decontamination process conformed to the Langmuir kinetic model, evidenced by the data's good fit to a single exponential decay function, as shown in te (Figure 4).

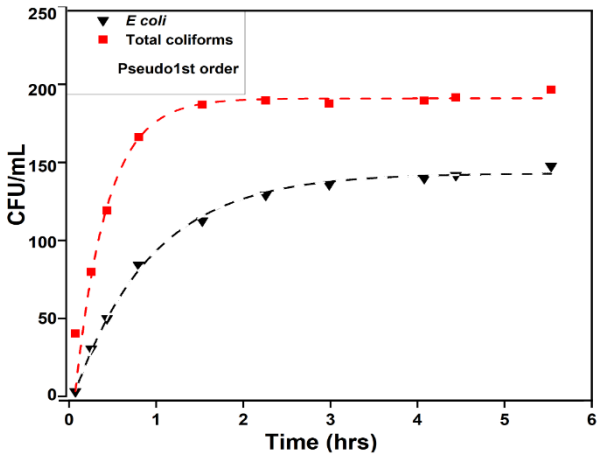

Fig. 5. Antibacterial kinetic curves for E. coli and T.coliforms degradation (CFU/mL) of bacterial cells.

The rate constants (K_2) were determined at various time intervals and were subject to non-linear curve fitting in Figure 4, with the corresponding R^2 values provided in Table 3. These high regression factors indicate that the decontamination adhered closely to the standard kinetics described by the Langmuir model, confirming the efficiency and predictability of the AC-FeS in bacterial removal under these conditions.

Table 3. Langmuir constants for antibacterial activity of gram-negative bacteria on activated Carbons.

Modified AC	CFU (mL)	Qmax (mg/g)	K_2	R^2
AC-FeS	T. coliforms	199	0.41	0.98
	E. coli	148	0.20	0.99

4. Conclusion

In this study, we successfully prepared hierarchical activated carbons (ACs) with micro and mesoporous texture and a very high surface area (1460 m^2/g). The AC was then post synthetically immobilized with FeS nanoparticles to afford AC-FeS. Detailed material characterization confirmed the incorporation of FeS, along with the presence of O^{2-} and OH^{-1} functionalities (through IR). This material demonstrated remarkable efficiency in removing F^-, NO_3^-, and decontamination activity of gram-negative bacteria from drinking water. The optimized removal achieved were 90% and 94% for NO_3^- and F^-, respectively, using FeS and AC-FeS in water sample. In contrast, AC-1 showed only minimal de-ionization activity. Notably, the material achieved complete (100%) bacterial removal within 6 hours. The findings of this research indicate a promising approach for the removal of both microbial and inorganic pollutants from drinking water, thereby contributing significantly to water purification technology.

Acknowledgements

The authors extend their appreciation to the Department of Chemistry, University of Azad Jammu and Kashmir, and the Environmental protection agency AJK, Pakistan. The authors are also thankful to Dr Muhammad Naeem Iqbal Department of Materials and Environmental Chemistry (MMK) at Stockholm University, Sweden for their logistics and technical support. The authors are also thankful to Dr Latif Ullah Khan, Department of Materials and Environmental Chemistry (MMK) at Stockholm University, Sweden for his inputs and technical support.

Data availability statement

The raw data is made available on request.

Conflict of Interest Statement

The authors declare no conflicts of competing interests.

References

[1] Elfiky, A.A.E.A.; Mubarak, M.F.; Keshawy, M.; Sayed, I.E.T.E.; Moghny, T.A.J.E., Development; Sustainability. Novel nanofiltration membrane modified by metal oxide nanocomposite for dyes removal from wastewater. 2024, 26, 19935-19957; https://doi.org/10.1007/s10668-023-03444-1

[2] Presley, S.M.; Rainwater, T.R.; Austin, G.P.; Platt, S.G.; Zak, J.C.; Cobb, G.P.; Marsland, E.J.; Tian, K.; Zhang, B.; Anderson, T.A.J.E.S.; et al. Assessment of pathogens and toxicants in New Orleans, LA following Hurricane Katrina. 2006, 40, 468-474; https://doi.org/10.1021/es052219p

[3] Boretti, A.; Rosa, L.J.N.C.W. Reassessing the projections of the world water development report. 2019, 2, 15; https://doi.org/10.1038/s41545-019-0039-9

[4] Gleick, P.H. Dirty-water: estimated deaths from water-related diseases 2000-2020; Citeseer: 2002.

[5] Shannon, M.A.; Bohn, P.W.; Elimelech, M.; Georgiadis, J.G.; Marinas, B.J.; Mayes, A.M.J.N.; Journals, t.a.c.o.r.f.n. Science and technology for water purification in the coming decades. 2010, 337-346; https://doi.org/10.1142/9789814287005_0035

[6] Leclerc, H.; Schwartzbrod, L.; Dei-Cas, E.J.C.r.i.m. Microbial agents associated with waterborne diseases. 2002, 28, 371-409; https://doi.org/10.1080/1040-840291046768

[7] Liang, L.; Xi, F.; Tan, W.; Meng, X.; Hu, B.; Wang, X.J.B. Review of organic and inorganic pollutants removal by biochar and biochar-based composites. 2021, 3, 255-281; https://doi.org/10.1007/s42773-021-00101-6

[8] Durner, E.F.; Poling, E.B.; Maas, J.L.J.H. Recent advances in strawberry plug transplant technology. 2002, 12, 545-550; https://doi.org/10.21273/HORTTECH.12.4.545

[9] Qi, L.; Xu, Z.; Jiang, X.; Hu, C.; Zou, X.J.C.r. Preparation and antibacterial activity of chitosan nanoparticles. 2004, 339, 2693-2700; https://doi.org/10.1016/j.carres.2004.09.007

[10] Lok, C.-N.; Ho, C.-M.; Chen, R.; He, Q.-Y.; Yu, W.-Y.; Sun, H.; Tam, P.K.-H.; Chiu, J.-F.; Che, C.-M.J.J.o.p.r. Proteomic analysis of the mode of antibacterial action of silver nanoparticles. 2006, 5, 916-924; https://doi.org/10.1021/pr0504079

[11] Akhavan, O.J.J.o.c.; science, i. Lasting antibacterial activities of Ag-TiO2/Ag/a-TiO2 nanocomposite thin film photocatalysts under solar light irradiation. 2009, 336, 117-124; https://doi.org/10.1016/j.jcis.2009.03.018

[12] Hu, W.; Peng, C.; Luo, W.; Lv, M.; Li, X.; Li, D.; Huang, Q.; Fan, C.J.A.n. Graphene-based antibacterial paper. 2010, 4, 4317-4323; https://doi.org/10.1021/nn101097v

[13] Agnihotri, S.; Mohan, T.; Jha, D.; Gautam, H.K.; Roy, I.J.A.o. Dual modality FeS nanoparticles with reactive oxygen species-induced and photothermal toxicity toward pathogenic bacteria. 2020, 5, 597-602; https://doi.org/10.1021/acsomega.9b03177

[14] Bhatnagar, A.; Sillanpää, M.J.C.e.j. Utilization of agro-industrial and municipal waste materials as potential adsorbents for water treatment-a review. 2010, 157, 277-296; https://doi.org/10.1016/j.cej.2010.01.007

[15] Kumar, S.; Ahlawat, W.; Bhanjana, G.; Heydarifard, S.; Nazhad, M.M.; Dilbaghi, N.J.J.o.n.; nanotechnology. Nanotechnology-based water treatment strategies. 2014, 14, 1838-1858; https://doi.org/10.1166/jnn.2014.9050

[16] Li, Q.; Mahendra, S.; Lyon, D.Y.; Brunet, L.; Liga, M.V.; Li, D.; Alvarez, P.J.J.W.r. Antimicrobial nanomaterials for water disinfection and microbial control: potential applications and implications. 2008, 42, 4591-4602; https://doi.org/10.1016/j.watres.2008.08.015

[17] Elkady, M.; Shokry, H.; Hamad, H.J.M. New activated carbon from mine coal for adsorption of dye in simulated water or multiple heavy metals in real wastewater. 2020, 13, 2498; https://doi.org/10.3390/ma13112498

[18] Muniandy, L.; Adam, F.; Mohamed, A.R.; Ng, E.-P.J.M.; Materials, M. The synthesis and characterization of high purity mixed microporous/mesoporous activated carbon from rice husk using chemical activation with NaOH and KOH. 2014, 197, 316-323; https://doi.org/10.1016/j.micromeso.2014.06.020

[19] Yang, K.; Peng, J.; Srinivasakannan, C.; Zhang, L.; Xia, H.; Duan, X.J.B.t. Preparation of high surface area activated carbon from coconut shells using microwave heating. 2010, 101, 6163-6169; https://doi.org/10.1016/j.biortech.2010.03.001

[20] Sjostrom, S.; Durham, M.; Bustard, C.J.; Martin, C.J.F. Activated carbon injection for mercury control: overview. 2010, 89, 1320-1322; https://doi.org/10.1016/j.fuel.2009.11.016

[21] Chen, Y.; Liang, W.; Li, Y.; Wu, Y.; Chen, Y.; Xiao, W.; Zhao, L.; Zhang, J.; Li, H.J.C.E.J. Modification, application and reaction mechanisms of nano-sized iron sulfide particles for pollutant removal from soil and water: A review. 2019, 362, 144-159; https://doi.org/10.1016/j.cej.2018.12.175

[22] Bagotia, N.; Sharma, A.K.; Kumar, S.J.C. A review on modified sugarcane bagasse biosorbent for removal of dyes. 2021, 268, 129309; https://doi.org/10.1016/j.chemosphere.2020.129309

[23] Demiral, H.; Gündüzoğlu, G.J.B.t. Removal of nitrate from aqueous solutions by activated carbon prepared from sugar beet bagasse. 2010, 101, 1675-1680; https://doi.org/10.1016/j.biortech.2009.09.087

[24] Yadav, A.K.; Abbassi, R.; Gupta, A.; Dadashzadeh, M.J.E.e. Removal of fluoride from aqueous solution and groundwater by wheat straw, sawdust and activated bagasse carbon of sugarcane. 2013, 52, 211-218; https://doi.org/10.1016/j.ecoleng.2012.12.069

[25] Sahu, J.; Karri, R.R.; Zabed, H.M.; Shams, S.; Qi, X.J.S.; Reviews, P. Current perspectives and future prospects of nano-biotechnology in wastewater treatment. 2021, 50, 139-158; https://doi.org/10.1080/15422119.2019.1630430

[26] Manceau, A.; Lanson, M.; Geoffroy, N.J.G.e.C.A. Natural speciation of Ni, Zn, Ba, and As in ferromanganese coatings on quartz using X-ray fluorescence, absorption, and diffraction. 2007, 71, 95-128; https://doi.org/10.1016/j.gca.2006.08.036

[27] Hamza, M.F.; Fouda, A.; Wei, Y.; El Aassy, I.E.; Alotaibi, S.H.; Guibal, E.; Mashaal, N.M.J.C.E.J. Functionalized biobased composite for metal decontamination-Insight on uranium and application to water samples collected from wells in mining areas (Sinai, Egypt). 2022, 431, 133967; https://doi.org/10.1016/j.cej.2021.133967

[28] Bouwer, H.J.A.w.m. Integrated water management: emerging issues and challenges. 2000, 45, 217-228; https://doi.org/10.1016/S0378-3774(00)00092-5

[29] Wei, R.P.; Liao, C.-M.; Gao, M.J.M.; A, M.T. A transmission electron microscopy study of constituent-particle-induced corrosion in 7075-T6 and 2024-T3 aluminum alloys. 1998, 29, 1153-1160; https://doi.org/10.1007/s11661-998-0241-8

[30] Jagtoyen, M.; Derbyshire, F.J.C. Activated carbons from yellow poplar and white oak by H3PO4 activation. 1998, 36, 1085-1097; https://doi.org/10.1016/S0008-6223(98)00082-7

[31] Jawad, A.H.; Abdulhameed, A.S.J.E., Ecology; Environment. Statistical modeling of methylene blue dye adsorption by high surface area mesoporous activated carbon from bamboo chip using KOH-assisted thermal activation. 2020, 5, 456-469; https://doi.org/10.1007/s40974-020-00177-z

[32] Fan, Z.; Zhang, Z.; Zhang, G.; Qin, L.; Fang, J.; Tao, P.J.I.J.o.E.S.; Technology. Phosphoric acid/FeCl3 converting waste mangosteen peels into bio-carbon adsorbents for methylene blue removal. 2022, 19, 12315-12328; https://doi.org/10.1007/s13762-022-03952-z

[33] Budinova, T.; Ekinci, E.; Yardim, F.; Grimm, A.; Björnbom, E.; Minkova, V.; Goranova, M.J.F.p.t. Characterization and application of activated carbon produced by H3PO4 and water vapor activation. 2006, 87, 899-905; https://doi.org/10.1016/j.fuproc.2006.06.005

[34] Srinivasan, N.; Shankar, P.; Bandyopadhyaya, R.J.C. Plasma treated activated carbon impregnated with silver nanoparticles for improved antibacterial effect in water disinfection. 2013, 57, 1-10; https://doi.org/10.1016/j.carbon.2013.01.008

[35] Mianowski, A.; Radko, T.; Siudyga, T.J.R.K., Mechanisms; Catalysis. Kinetic compensation effect of isoconversional methods. 2021, 132, 37-58; https://doi.org/10.1007/s11144-020-01898-2

[36] Liu, S.; Zeng, T.H.; Hofmann, M.; Burcombe, E.; Wei, J.; Jiang, R.; Kong, J.; Chen, Y.J.A.n. Antibacterial activity of graphite, graphite oxide, graphene oxide, and reduced graphene oxide: membrane and oxidative stress. 2011, 5, 6971-6980; https://doi.org/10.1021/nn202451x

[37] Gurunathan, S.; Han, J.W.; Dayem, A.A.; Eppakayala, V.; Kim, J.-H.J.I.j.o.n. Oxidative stress-mediated antibacterial activity of graphene oxide and reduced graphene oxide in Pseudomonas aeruginosa. 2012, 7, 5901; https://doi.org/10.2147/IJN.S37397

[38] Tian, Y.; Qi, J.; Zhang, W.; Cai, Q.; Jiang, X.J.A.a.m.; interfaces. Facile, one-pot synthesis, and antibacterial activity of mesoporous silica nanoparticles decorated with well-dispersed silver nanoparticles. 2014, 6, 12038-12045; https://doi.org/10.1021/am5026424

[39] Dizaj, S.M.; Lotfipour, F.; Barzegar-Jalali, M.; Zarrintan, M.H.; Adibkia, K.J.M.S.; C, E. Antimicrobial activity of the metals and metal oxide nanoparticles. 2014, 44, 278-284; https://doi.org/10.1016/j.msec.2014.08.031

[40] Park, S.-J.; Jang, Y.-S.J.J.o.c.; science, i. Preparation and characterization of activated carbon fibers supported with silver metal for antibacterial behavior. 2003, 261, 238-243; https://doi.org/10.1016/S0021-9797(03)00083-3

[41] Oya, A.; Yoshida, S.; Alcaniz-Monge, J.; Linares-Solano, A.J.c. Preparation and properties of an antibacterial activated carbon fiber containing mesopores. 1996, 34, 53-57; https://doi.org/10.1016/0008-6223(95)00134-4

[42] Zhang, S.; Fu, R.; Wu, D.; Xu, W.; Ye, Q.; Chen, Z.J.C. Preparation and characterization of antibacterial silver-dispersed activated carbon aerogels. 2004, 42, 3209-3216; https://doi.org/10.1016/j.carbon.2004.08.004

[43] Mutalik, C.; Okoro, G.; Krisnawati, D.I.; Jazidie, A.; Rahmawati, E.Q.; Rahayu, D.; Hsu, W.-T.; Kuo, T.-R.J.J.o.C.; Science, I. Copper sulfide with morphology-dependent photodynamic and photothermal antibacterial activities. 2022, 607, 1825-1835; https://doi.org/10.1016/j.jcis.2021.10.019

[44] Xu, N.; Huang, Q.; Shi, L.; Wang, J.; Li, X.; Guo, W.; Yan, D.; Ni, T.; Yang, Z.; Yan, Y.J.D.T. A bioinspired polydopamine-FeS nanocomposite with high antimicrobial efficiency via NIR-mediated Fenton reaction. 2023, 52, 1687-1701; https://doi.org/10.1039/D2DT03765C

[45] Awwad, A.M.; Salem, N.M.; Aqarbeh, M.M.; Abdulaziz, F.M.J.C.I. Green synthesis, characterization of silver sulfide nanoparticles and antibacterial activity evaluation. 2020, 6, 42-48.

[46] Pachaiappan, R.; Cornejo-Ponce, L.; Rajendran, R.; Manavalan, K.; Femilaa Rajan, V.; Awad, F.J.B. A review on biofiltration techniques: Recent advancements in the removal of volatile organic compounds and heavy metals in the treatment of polluted water. 2022, 13, 8432-8477; https://doi.org/10.1080/21655979.2022.2050538

[47] Li, X.; Xu, H.; Chen, Z.-S.; Chen, G.J.J.o.n. Biosynthesis of nanoparticles by microorganisms and their applications. 2011, 2011, 1-16; https://doi.org/10.1155/2011/270974

[48] Ajibade, F.O.; Akosile, S.I.; Oluwatuyi, O.E.; Ajibade, T.F.; Lasisi, K.H.; Adewumi, J.R.; Babatola, J.O.; Oguntuase, A.M.J.R.i.E. Bacteria removal efficiency data and properties of Nigerian clay used as a household ceramic water filter. 2019, 2, 100011; https://doi.org/10.1016/j.rineng.2019.100011

[49] Demiral, İ.; Samdan, C.; Demiral, H.J.S.; Interfaces. Enrichment of the surface functional groups of activated carbon by modification method. 2021, 22, 100873; https://doi.org/10.1016/j.surfin.2020.100873

[50] Wang, X.; Cheng, H.; Ye, G.; Fan, J.; Yao, F.; Wang, Y.; Jiao, Y.; Zhu, W.; Huang, H.; Ye, D.J.C. Key factors and primary modification methods of activated carbon and their application in adsorption of carbon-based gases: A review. 2022, 287, 131995; https://doi.org/10.1016/j.chemosphere.2021.131995

[51] Wang, W.; Cheng, X.; Liao, J.; Lin, Z.; Chen, L.; Liu, D.; Zhang, T.; Li, L.; Lu, Y.; Xia, H.J.A.B.S.; et al. Synergistic photothermal and photodynamic therapy for effective implant-related bacterial infection elimination and biofilm disruption using Cu9S8 nanoparticles. 2019, 5, 6243-6253.

[52] Hsueh, Y.-H.; Tsai, P.-H.; Lin, K.-S.; Ke, W.-J.; Chiang, C.-L.J.J.o.n. Antimicrobial effects of zero-valent iron nanoparticles on gram-positive Bacillus strains and gram-negative Escherichia coli strains. 2017, 15, 1-12. https://doi.org/10.1186/s12951-017-0314-1

[53] Hossain, N.; Nizamuddin, S.; Ball, A.S.; Shah, K.J.P.S.; Protection, E. Synthesis, performance and reaction mechanisms of Ag-modified multi-functional rice husk solvochar for removal of multi-heavy metals and water-borne bacteria from wastewater. 2024, 182, 56-70; https://doi.org/10.1016/j.psep.2023.11.058

[54] Singh, N.; Singh, R.; Shah, K.; Pramanik, B.K.J.C. Green synthesis of zinc oxide nanoparticles using lychee peel and its application in anti-bacterial properties and CR dye removal from wastewater. 2023, 327, 138497; https://doi.org/10.1016/j.chemosphere.2023.138497

[55] Zhang, H.; Wang, C.; Luo, H.; Chen, J.; Kuang, M.; Yang, J.J.A.C. Iron Nanoparticles Protected by Chainmail-structured Graphene for Durable Electrocatalytic Nitrate Reduction to Nitrogen. 2023, 135, e202217071; https://doi.org/10.1002/ange.202217071

[56] Kahya, N.; Erim, F.B.J.I.J.o.B.M. Removal of fluoride ions from water by cerium-carboxymethyl cellulose beads doped with CeO2 nanoparticles. 2023, 242, 124595; https://doi.org/10.1016/j.ijbiomac.2023.124595